



## Differentiation between malignancy and inflammation in pulmonary ground-glass nodules: The feasibility of integrated $^{18}\text{F}$ -FDG PET/CT

Eun Ju Chun<sup>a</sup>, Hyun Ju Lee<sup>b,\*</sup>, Won Jun Kang<sup>c</sup>, Kwang Gi Kim<sup>d</sup>,  
Jin Mo Goo<sup>b</sup>, Chang Min Park<sup>b</sup>, Chang Hyun Lee<sup>b</sup>

<sup>a</sup> Department of Radiology, Seoul National University Bundang Hospital, Republic of Korea

<sup>b</sup> Department of Radiology, Institute of Radiation Medicine and Clinical Research Institute, Seoul National University Hospital, 101 Daehangno, 28 Yeongseon-dong, Jongno-gu, Seoul 110-744, Republic of Korea

<sup>c</sup> Division of Nuclear Medicine, Department of Radiology, Yonsei University College of Medicine, Republic of Korea

<sup>d</sup> Department of Medical Engineering, National Cancer Center, Republic of Korea

### ARTICLE INFO

#### Article history:

Received 6 October 2008

Received in revised form 17 November 2008

Accepted 20 November 2008

#### Keywords:

Ground-glass nodule

Ground-glass opacity

GGN

GGO

Solitary pulmonary nodules

PET/CT

$^{18}\text{F}$ -FDG

### ABSTRACT

**Background:**  $^{18}\text{F}$ -FDG PET/CT has been used to differentiate malignant solid lung nodules from benign nodules. We assess the feasibility of integrated  $^{18}\text{F}$ -FDG PET/CT for the differentiation of malignancy from inflammation manifested as ground-glass nodules (GGNs) on chest CT.

**Methods:** A total of 68 GGNs in 45 patients (M:F = 24:21; mean age, 61) fulfilled the following criteria: (a) nodules composed of  $\geq 50\%$  ground-glass opacity, (b) patients who underwent integrated PET/CT within 1 week following dedicated chest CT, (c) definitive diagnosis determined by pathological specimen or at least 9 months of follow-up, and (d) lesions  $\geq 10$  mm in diameter. 36 malignant GGNs were pathologically proved as adenocarcinoma ( $n = 20$ ), bronchioloalveolar carcinoma ( $n = 11$ ), low-grade lymphoma ( $n = 3$ ), metastatic mucinous adenocarcinoma ( $n = 1$ ) and unknown low-grade malignancy ( $n = 1$ ). 32 inflammatory GGNs were confirmed as pneumonic infiltration as they had disappeared on follow-up CT and were associated with compatible clinical features ( $n = 26$ ) or as chronic inflammation with fibrosis by VATS biopsy ( $n = 6$ ). Using CT density histogram analysis, 14 were classified as pure GGNs and 54 as part-solid nodules. Integrated PET/CT was evaluated by measuring the maximum standardized uptake value (SUV) at the region of interest located at each lesion. The Mann–Whitney  $U$  test was performed to compare the SUV of malignancy and inflammation. The optimal cut-off value of SUV to differentiate malignancy from inflammation was determined using a receiver operating characteristic-based positive test. Sensitivity, specificity, accuracy, and positive predictive values (PPV) and negative predictive values (NPV) were calculated at the level of the optimal cut-off value. SUV showing 100% PPV for inflammatory GGNs was evaluated.

**Results:** In part-solid nodules, the maximum SUV was significantly higher in inflammation ( $2.00 \pm 1.18$ ; range, 0.48–5.60) than in malignancy ( $1.26 \pm 0.71$ ; range, 0.32–2.6) ( $P = 0.018$ ). On the other hand, in pure GGNs, the maximum SUV of malignancy ( $0.64 \pm 0.19$ ; range, 0.43–0.96) and inflammation ( $0.74 \pm 0.28$ ; range, 0.32–1.00) showed no difference ( $P = 0.37$ ). Using the optimal cut-off value of SUV as 1.2 ( $P = 0.01$ ) sensitivity, specificity, accuracy, PPV and NPV in part-solid nodules were 62.1%, 80.0%, 70.4%, 78.3% and 64.5%, respectively. Six part-solid nodules, which showed a maximum SUV of higher than 2.6, were all inflammations.

**Conclusion:** The part-solid nodules with positive FDG-PET could be inflammatory nodules rather than malignant nodules. This is a quite paradoxical result when considering the basic knowledge that malignant pulmonary nodules have higher glucose metabolism.

© 2008 Elsevier Ireland Ltd. All rights reserved.

### 1. Introduction

Positron emission tomography (PET) with F-18 fludeoxyglucose ( $^{18}\text{F}$ -FDG) has been used to differentiate malignant from benign lesions due to high isotope uptake secondary to the increased metabolic activity of malignant lesions compared to benign lesions. There have been many reports relating the

\* Corresponding author. Tel.: +82 2 2072 1861; fax: +82 2 743 6385.

E-mail address: [rosaceci@radiol.snu.ac.kr](mailto:rosaceci@radiol.snu.ac.kr) (H.J. Lee).

usefulness of  $^{18}\text{F}$ -FDG PET in differentiating malignant pulmonary nodules from benign nodules [1–3]. However, these reports were focused on solitary pulmonary nodules and did not consider the morphologic characteristics of nodules such as solid or ground-glass opacities. A ground-glass nodule (GGN) was defined as less dense pulmonary nodules that did not obscure pulmonary vasculature. Recently, GGNs have been getting a lot of attention due to its higher malignant potential. According to the Early Lung Cancer Action Program (ELCAP) study, 20% of pulmonary nodules on baseline screening were GGNs [4]. This study demonstrated that the overall frequency of malignancy is much higher in GGNs than in solid nodules.

It is well known that bronchioloalveolar carcinoma (BAC), which typically manifests as GGN, exhibits little uptake on  $^{18}\text{F}$ -FDG PET, though it is classified as malignancy [5]. In contrast, some benign inflammatory or infectious conditions such as pneumocystis carinii pneumonia or eosinophilic pneumonia, which often manifested as GGN, were reported to have high glucose uptake on  $^{18}\text{F}$ -FDG PET scan [6,7]. However, to our knowledge, there have been no reports of a comprehensive comparison of  $^{18}\text{F}$ -FDG PET findings between benign and malignant GGNs. Therefore, the aim of this study was to assess whether integrated  $^{18}\text{F}$ -FDG PET/CT can assist in the differentiation of malignant GGNs from benign GGNs.

## 2. Materials and methods

Approval for this study was obtained from our institutional review board. The requirement for informed consent was waived.

### 2.1. Selection of ground-glass nodules

Patients were identified from a retrospective data search using the key words “ground-glass opacity,” “ground-glass nodule,” “nodular ground-glass attenuation,” “focal ground-glass opacity,” and “focal ground-glass attenuation,” from the CT database of Seoul National University Hospital from November 2003 to February 2006. A total of 68 GGNs in 45 patients (M:F = 24:21; mean age, 61 years) fulfilled the following conditions for inclusion: (a) nodules composed of  $\geq 50\%$  ground-glass opacity, (b) patients who underwent integrated  $^{18}\text{F}$ -FDG PET/CT within 1 week following chest CT, (c) definitive diagnosis determined by pathological specimen or at least 9 months of follow-up chest CT, in which a lesion that disappeared within the 9-month follow-up period was classified as inflammation, and (d) lesions showing a nodular appearance  $\geq 10$  mm in diameter so as to avoid the limitation of spatial resolution of current generation  $^{18}\text{F}$ -FDG PET/CT scanners.

Among the 68 GGNs, 36 were malignant tumors and 32 were inflammatory lesions. All malignant GGNs were pathologically confirmed as adenocarcinoma ( $n = 20$ ), BAC ( $n = 11$ ), low-grade lymphoma ( $n = 3$ ), metastasis from mucinous adenocarcinoma ( $n = 1$ ), and unknown low-grade malignancy ( $n = 1$ ). Inflammatory GGNs were confirmed as chronic inflammation with fibrosis by VATS resection ( $n = 6$ ) or were considered to be pneumonic infiltration due to their disappearance on follow-up CT ( $n = 26$ ). Among the 26 pneumonic infiltrations, four GGNs in three patients were assumed to be simple eosinophilic pneumonia, as the lesions were found in the period of hypereosinophilia and had disappeared after normalization of peripheral eosinophil count.

### 2.2. Chest CT: imaging protocol and nodule characterization

Chest CT was performed with Sensation-16 (Siemens Medical Systems, Erlangen, Germany), Lightspeed Ultra (GE Medical Systems, Milwaukee, WI, USA) and Mx8000 (Philips Medical Systems, Best, The Netherlands) with 120 kVp, 150–200 mAs, pitch of

0.875–1.5, and collimation of 1–2.5 mm. Images were reconstructed using the high frequency algorithm with 1–5 mm thickness. CT scans were obtained for all patients in the supine position at full inspiration.

GGNs were categorized into pure GGNs and part-solid nodules using CT density histograms as reported earlier [8,9]. Two board-certified radiologists (E.J.C., H.J.L.; 10 and 11 years of experience in chest imaging) selected the CT section in each lesion that demonstrated the largest cross-sectional area of the GGN. CT images were displayed using a lung window with a center of  $-700$  HU and a width of 1500 HU. One of the two radiologists (E.J.C.) outlined the boundary of each GGN on soft-copy CT images using an in-house graphic user interface. A histogram was created from the CT numbers of each pixel within the lesion. When only one peak of CT number histogram was found between  $-800$  and  $-400$  HU, the lesion was categorized as pure GGN (Fig. 1). When the first peak was located between  $-800$  and  $-400$  HU and the second peak was between  $-150$  and  $50$  HU, the lesion was categorized as part-solid nodule (Fig. 2). In this manner, 14 lesions were classified as pure GGNs and 54 were classified as part-solid nodules. Among the 14

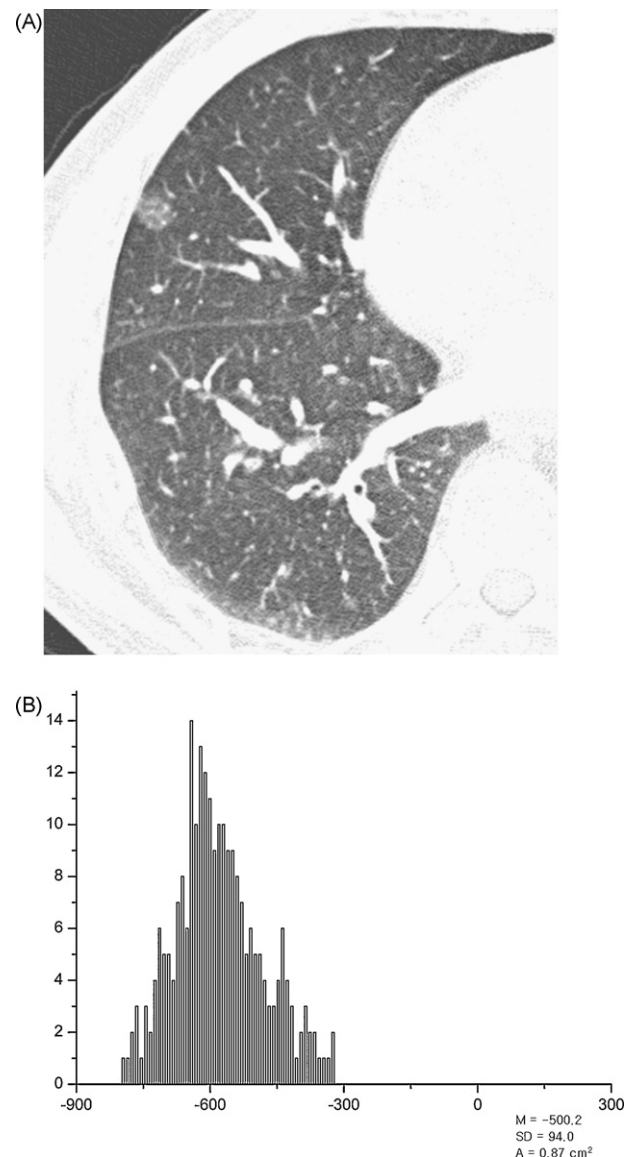


**Fig. 1.** CT number histogram of a pure ground-glass nodule. (A) Chest CT shows a pulmonary nodule manifesting as homogenous ground-glass opacity in the right middle lobe. (B) CT number histogram shows one peak at  $-620$  HU.

Download English Version:

<https://daneshyari.com/en/article/2143186>

Download Persian Version:

<https://daneshyari.com/article/2143186>

[Daneshyari.com](https://daneshyari.com)